RESEARCH ARTICLE

A Novel SNCA A30G Mutation Causes Familial Parkinson's Disease

Hui Liu, MSc,[1] Christos Koros, MD, PhD,[2,3] Timo Strohäker, PhD,[4] Claudia Schulte, MSc,[1] Maria Bozi, MD, PhD,[3] Stefanos Varvaresos, MD,[2] Alain Ibáñez de Opakua, PhD,[4] Athina Maria Simitsi, MD, MSc,[2] Anastasia Bougea, MD, PhD,[2] Konstantinos Voumvourakis, MD, PhD,[3] Matina Maniati, PhD,[5] Sokratis G. Papageorgiou, MD, PhD,[2,3] Ann-Kathrin Hauser,[1] Stefan Becker, PhD,[6] Markus Zweckstetter, PhD,[4,6*] Leonidas Stefanis, MD, PhD,[2,5*] and Thomas Gasser, MD, PhD[1*]

[1]*Department for Neurodegenerative Diseases, Hertie Institute for Clinical Brain Research, University of Tübingen and German Center of Neurodegenerative Diseases (DZNE), Tübingen, Germany*
[2]*1st Department of Neurology, Eginition Hospital, National and Kapodistrian University of Athens, Athens, Greece*
[3]*2nd Department of Neurology, Attikon Hospital, National and Kapodistrian University of Athens, Athens, Greece*
[4]*German Center for Neurodegenerative Diseases (DZNE), Göttingen, Germany*
[5]*Laboratory of Neurodegenerative Diseases, Biomedical Research Foundation of the Academy of Athens, Athens, Greece*
[6]*Department for NMR-based Structural Biology, Max Planck Institute for Biophysical Chemistry, Göttingen, Germany*

ABSTRACT: Background: The SNCA gene encoding α-synuclein (αSyn) is the first gene identified to cause autosomal-dominant Parkinson's disease (PD).
Objective: We report the identification of a novel heterozygous A30G mutation of the SNCA gene in familial PD and describe clinical features of affected patients, genetic findings, and functional consequences.
Methods: Whole exome sequencing was performed in the discovery family proband. Restriction digestion with BbvI was used to screen SNCA A30G in two validation cohorts. The Greek cohort included 177 familial PD probands, 109 sporadic PD cases, and 377 neurologically healthy controls. The German cohort included 136 familial PD probands, 380 sporadic PD cases, and 116 neurologically healthy controls. We also conducted haplotype analysis using 13 common single nucleotide variants around A30G to determine the possibility of a founder effect for A30G. We then used biophysical methods to characterize A30G αSyn.
Results: We identified a novel SNCA A30G (GRCh37, Chr4:90756730, c.89 C>G) mutation that co-segregated with the disease in five affected individuals of three Greek families and was absent from controls. A founder effect was strongly suggested by haplotype analysis. The A30G mutation had a local effect on the intrinsically disordered structure of αSyn, slightly perturbed membrane binding, and promoted fibril formation.
Conclusion: Based on the identification of A30G co-segregating with the disease in three families, the absence of the mutation in controls and population databases, and the observed functional effects, we propose SNCA A30G as a novel causative mutation for familial PD.

Key Words: Parkinson's disease; SNCA; A30G

[The copyright line for this article was changed on 02 April 2021, after original online publication.]

***Correspondence to:** Dr. Thomas Gasser, Department for Neurodegenerative Diseases, Hertie Institute for Clinical Brain Research, University of Tübingen and German Center for Neurodegenerative Diseases (DZNE), Tübingen, Germany; E-mail: thomas.gasser@uni-tuebingen.de or Dr. Markus Zweckstetter, German Center for Neurodegenerative Diseases (DZNE), Göttingen, Germany. Email: Markus.Zweckstetter@dzne.de or Dr. Leonidas Stefanis, 2nd Department of Neurology, Attikon Hospital, National and Kapodistrian University of Athens, Athens, Greece. Email: lstefanis@bioacademy.gr

Hui Liu and Christos Koros share the first authorship and contributed equally to this article.

Leonidas Stefanis and Markus Zweckstetter contributed equally to this article.

Relevant conflicts of interest/financial disclosures: Nothing to report.

Funding agencies: This study was supported by the advanced grant "787679 - LLPS-NMR" of the European Research Council (to M.Z.), Hellenic Ministry of Education and Religion THALIS grant number 377206 (to L.S.), and by ongoing studies in familial PD cohorts supported by the Parkinson's Disease Progression Markers Initiative (PPMI).

Received: 1 December 2020; **Revised:** 15 January 2021; **Accepted:** 29 January 2021

Published online 22 February 2021 in Wiley Online Library (wileyonlinelibrary.com). DOI: 10.1002/mds.28534

Parkinson's disease (PD) is the most prevalent movement disorder and the second most common neurodegenerative disease characterized by cardinal motor symptoms and various non-motor symptoms.[1] The pathological hallmark of PD is the degeneration of nigrostriatal dopaminergic neurons and the widespread formation of Lewy bodies, which are abnormal neuronal cytoplasmic inclusions composed mostly of aggregated α-synuclein (αSyn), a widely expressed protein encoded by the SNCA gene.[2] SNCA is the first gene identified to cause autosomal dominant PD[3] and, to date, there are seven different missense mutations (A30P, E46K, H50Q, G51D, A53T, A53E, and A53V) reported to be associated with PD.

The A53T mutation, the first SNCA missense mutation identified, has been detected mainly in families of Greek-Italian descent.[4] The H50Q mutation was reported in one sporadic case[5] and one dominant family,[6] but it was later considered to be probably not pathogenic because there was no evident enrichment in PD cases compared to controls in large population databases.[7] The A53V mutation was found in one dominant Japanese family but in a homozygous state[8] and in one dominant family and two sporadic PD cases from China in a heterozygous state,[9] but it still needs more functional or pathological evidence to confirm whether homozygous or heterozygous A53V mutation can predispose carriers to PD. Other SNCA missense mutations (E46K,[10,11] G51D,[12,13] and A53E[14,15]) have been found in several families and/or cases, while A30P was only found to co-segregate in five affected cases of one German family.[16]

In the current study, we identified a novel heterozygous A30G mutation of the SNCA gene in five affected individuals of three Greek families not known to be related. Here we describe clinical features, genetic findings, and results of functional studies.

Methods

The Discovery Family

An autosomal dominant Greek family (Fig. 1a), including four affected cases (the proband, his brother, his father, and his aunt), was recruited. In the proband (III.2), known dominant PD-related mutations (SNCA A53T, LRRK2, and VPS35) were excluded by Sanger sequencing.

Validation Cohorts

We screened for SNCA A30G mutation in two different cohorts from Greece and Germany respectively. The Greek cohort included 177 probands with PD and a positive family history (age at onset [AAO] = 57.1 ± 13.2 years) of which 85 with dominant inheritance and 92 with undetermined inheritance pattern, 109 sporadic PD cases with an AAO at or below the age of 50 years (AAO = 42.6 ± 8.5 years) recruited from the 1st and 2nd Department of Neurology of the National and Kapodistrian University of Athens, and 377 neurologically healthy controls (age at examination = 60.9 ± 10.6 years). The German cohort included 136 PD probands (AAO = 57.5 ± 10.1 years) with a positive family history, 380 sporadic PD cases (AAO = 52.4 ± 8.9 years) recruited from University Hospital of Tübingen, and 116 neurologically healthy controls (age at examination = 62.4 ± 6.9 years).

PD was diagnosed based on the Movement Disorder Society (MDS) clinical diagnostic criteria.[17] This study was approved by the relevant ethical authorities, and all the subjects provided informed consent. Demographic and clinical data were collected. The Unified Parkinson's Disease Rating (UPDRS) Part III[18] and Hoehn and Yahr (H&Y) stage systems[19] were used to evaluate motor severity. Cognitive function was evaluated using the Montreal Cognitive Assessment (MoCA)[20] or Mini-Mental Status Examination (MMSE).[21]

Genetic Studies

Whole exome sequencing (WES) was performed on the discovery family (Fig. 1a) proband and variants were annotated with Variant Effect Predictor (VEP).[22] The potential pathogenicity of variants was predicted by Mutation Taster,[23] SIFT[24] and CADD.[25]

Sanger sequencing was used to confirm the A30G mutation (Fig. 2a). Multiplex Ligation-dependent Probe Amplification (MLPA) kit (P051 kit; MRC-Holland, Amsterdam, The Netherlands) was conducted to search for putative additional SNCA exon deletions or duplications.

For SNCA A30G mutation screening, restriction digestion was done with BbvI (R0173S) according to the manufacturer's protocol (New England Biolabs, Beverly, MA, USA). Mutant alleles carrying the C89G substitution were identified through the presence of 199 and 141 base pair (bp) digestion products (Fig. 2b).

To determine the possibility of a founder effect of the recurring A30G mutation in these families, 13 common single nucleotide variants (SNVs) around SNCA A30G (see Table S1) were directly sequenced after polymerase chain reaction (PCR) amplification in all available family members.

Biophysical Studies

Protein and liposome preparation, nuclear magnetic resonance (NMR) spectroscopy, molecular dynamics (MD) simulations, aggregation assay, fibril harvest, circular dichroism (CD) spectroscopy, dynamic light scattering, and transmission electron microscopy (TEM) were performed to analyze the functional consequences of the A30G mutation. Methods are described in the Supporting Information Methods.

Results

The Discovery Family: Co-Segregation of SNCA A30G

Four individuals across two generations were affected with PD (Fig. 1a). The AAO of the members in this

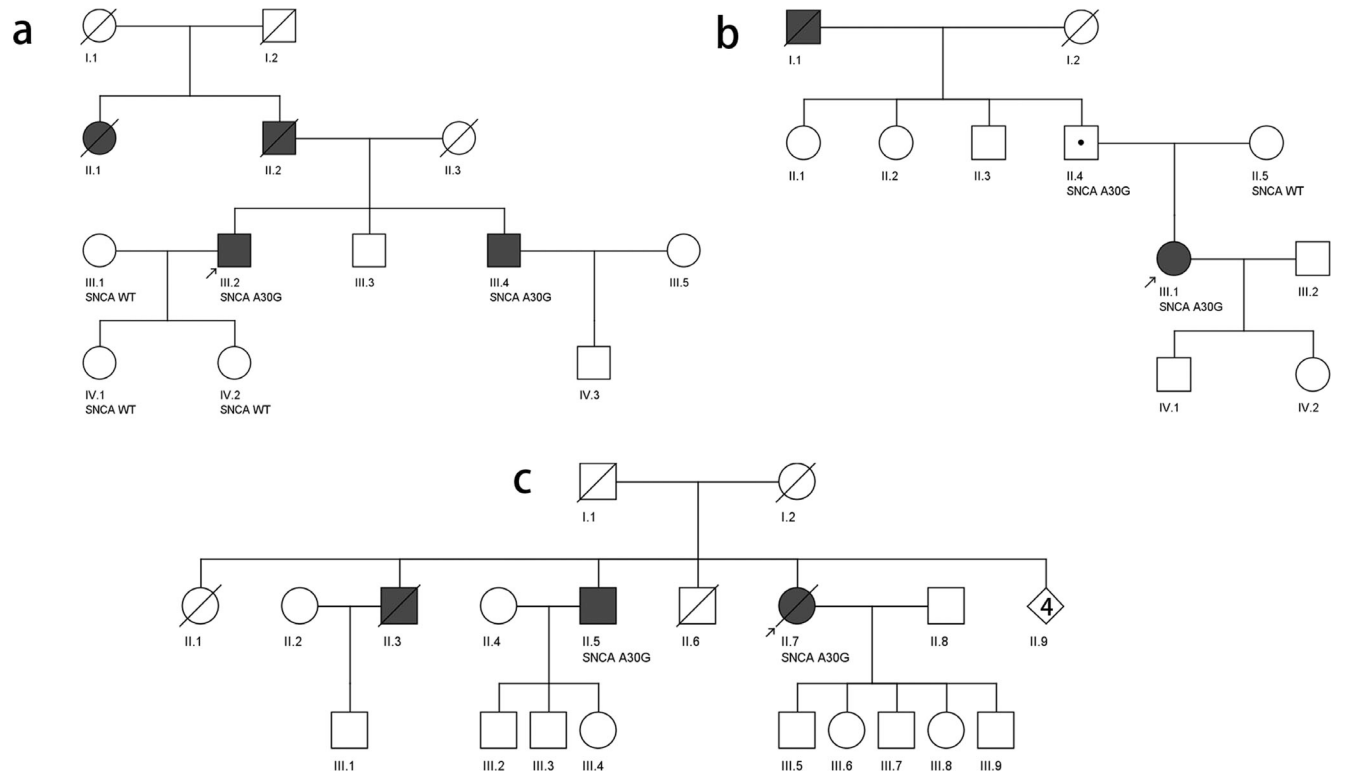

FIG. 1. Pedigrees of families with A30G mutation. Circles indicate females and squares indicate males. Affected individuals with Parkinson's disease (PD) are represented with black symbols and unaffected with open symbols. The open symbol with a dot refers to the individual carrying A30G but not meeting the PD diagnostic criteria. Individuals who are deceased have a slash through the symbol representing them. The diamond symbol with a number means the number of siblings. The arrow points to a proband in each family. WT denotes wild type. (**a**) The proband and his brother carry the A30G mutation. His wife and two daughters do not carry the mutation. (**b**) The proband and her father carry the A30G mutation. The father had mild motor symptoms, but did not meet the PD diagnostic criteria. The mother does not carry the A30G mutation. (**c**) The proband and her brother carry the A30G mutation. Another brother's DNA was not available.

family ranged from 43 to 65 years. The demographic and clinical features of the proband and the family members are summarized in Table S2.

The index case (III.2) was a male who manifested clinical PD, including rest tremor, rigidity, and bradykinesia. His first symptom was rest tremor of his left leg at age 43 years. He had a good initial response to levodopa treatment but gradually suffered from wearing-off, dyskinesia, freezing of gait, and falls. The disease duration at the time of evaluation was 6 years; at this time, he also suffered from various non-motor symptoms, including severe cognitive decline, depression, anxiety, apathy, disinhibition, mild visual hallucinations, rapid eye movement sleep behavior disorder (RBD), severe orthostatic hypotension, and urinary incontinence. In terms of neurological examination, the patient was clinically assessed as H&Y stage 3, with a UPDRS III score (off) of 39 and a score of 7/30 in MMSE.

The brother (III.4) of the proband developed upper limb rest tremor at age 57 years. With a relatively short disease duration (2 years), he only presented with mild motor dysfunction and was at a H&Y stage 1. His father and aunt had the same AAO of 65 years and died at the age of 84 and 75 years, respectively. Their clinical phenotype information included bradykinesia and rest tremor. His father also had dementia with onset at the age of 80 years.

WES analysis showed the SNCA A30G mutation was present in the proband (III.2). This mutation was not reported in public databases, including 1000 Genomes and GnomAD, and it was predicted as deleterious by all in silico prediction algorithms (Mutation Taster: disease-causing, SIFT: damaging 0.03, and CADD: 28.6). The SNCA A30 residue is highly conserved across most species (Fig. 2c). Screening for segregation of SNCA A30G in the family, it was found in his brother, but not in the three unaffected members in this family. DNA from the father and aunt of the index patient was not available. The variant was confirmed by PCR-Sanger sequencing in all the members (Figs 1a and 2a). No SNCA exon deletions or duplications were found in the A30G carriers.

Validation Cohorts: Two Additional PD Families with SNCA A30G Mutation

Using PCR, restriction digest, and confirmation with Sanger sequencing, we detected the SNCA A30G

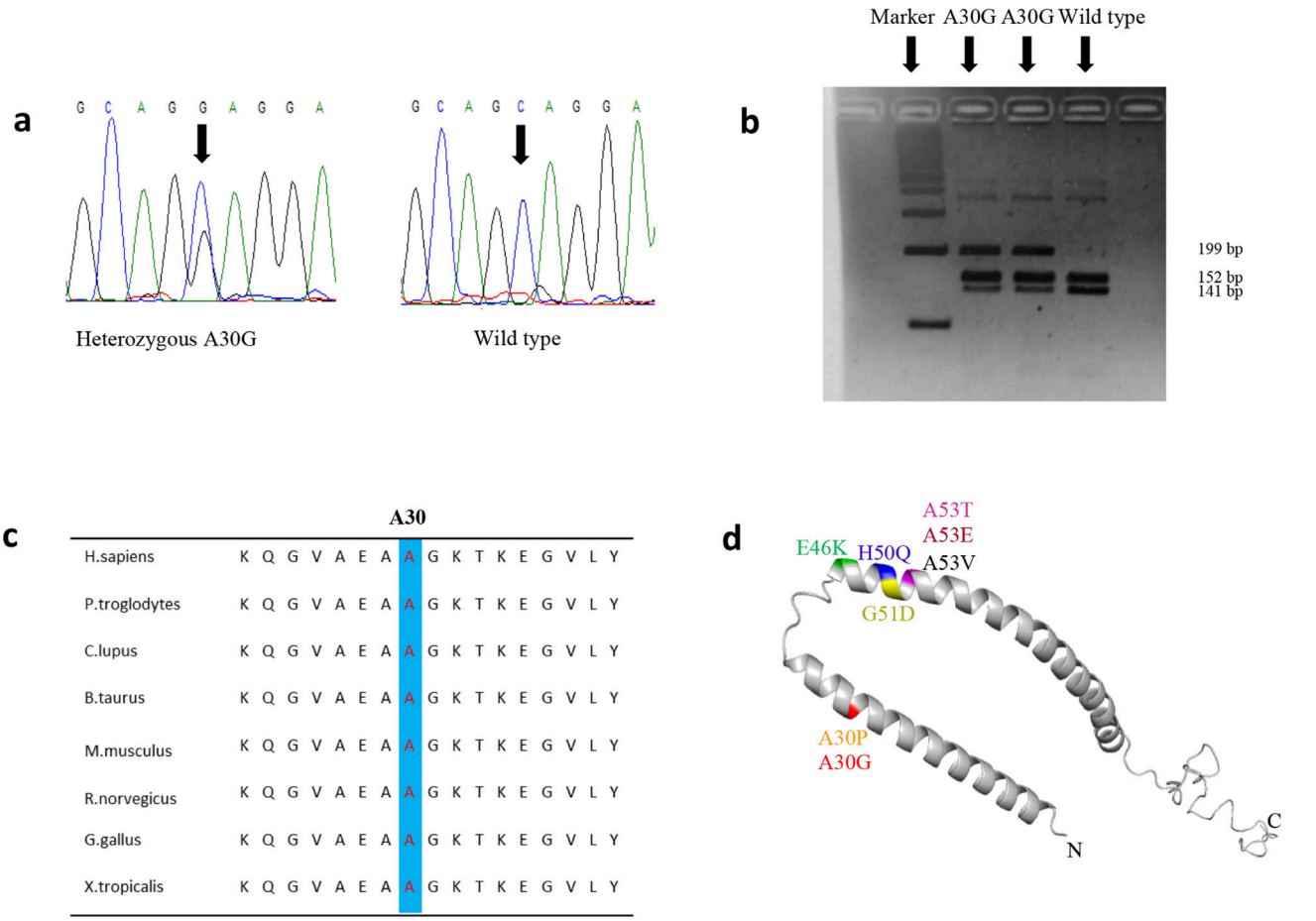

FIG. 2. Mutation screening, conservation of A30G and structure of α-synuclein (αSyn) with known mutations labeled. (**a**) Sanger sequence confirmation. The A30G mutation was present in affected Parkinson's disease cases and wild type (WT) was present in unaffected family members. (**b**) Restriction digestion. The digested products of A30G mutation and WT. (**c**) Conservation of the SNCA A30G missense mutation. Protein homologues were aligned using NCBI homolo gene (https://www.ncbi.nlm.nih.gov/homologene). (**d**) Three-dimensional vesicle-bound α-helical structure of αSyn (PDB ID: 1XQ8). Mutations are located within the N-terminal helical part. [Color figure can be viewed at wileyonlinelibrary.com]

mutation in three affected individuals of two additional Greek PD families (Fig. 1b,c). Again, no SNCA exon deletions or duplications were found in the A30G carriers. The mutation was not found in 377 unrelated Greek and 116 German control individuals.

In Family B (Fig. 1b), the proband (III.1) was an early-onset PD patient and her father also harbored the A30G mutation. At age 36 years, the proband developed right hand rigidity and bradykinesia. There was good initial levodopa response, but after only 3 years wearing-off developed. She also suffered from various non-motor symptoms, including depression, hallucinations, impulse control disorder, RBD, orthostatic hypotension, and urinary urgency. When the disease duration was 7 years, she was at a H&Y stage 2, scored 27 in UPDRS III (on), and scored 28/30 in MoCA. Due to motor fluctuations, she had subsequently undergone deep brain stimulation (DBS) treatment with an initial favorable response of 3 years. After 13 years of disease, the H&Y stage was 3 and the score for UPDRS III (on, under apomorphine pump treatment, which had been initiated 6 months earlier) and MoCA was 44 and 22/30, respectively. Her father, at age 80 years, experienced only mild stiffness of right upper limb, right leg rest tremor, with H&Y stage 1 and UPDRS III 11, and no bradykinesia, and thus did not meet the recently proposed MDS PD diagnostic criteria. However, he had cognitive decline, with MoCA 14/30 and various non-motor symptoms, such as severe depression, anxiety, psychotic features, and RBD. The grandfather of the index patient was diagnosed with PD at age 80 years and died at age 90 years.

In family C (Fig. 1c), the AAO of the three affected cases was similar, between 58 and 62 years. Both the proband (II.7) and her brother (II.5) were identified with SNCA A30G. The proband developed limb rest tremor at age 58 years with good response to levodopa. By age 65 years, she complained of wearing-off and examination revealed bradykinesia, rigidity, and postural instability. Cognitive decline, with MMSE 24/30, depression, orthostatic hypotension, and severe RBD, were also noted. The H&Y stage was 3 and the UPDRS III score (on) was 22. She died at age 67 years because

of sepsis and complications of diabetes mellitus. Her brother (II.5) developed bradykinesia at age 60 years with good initial response to levodopa. When evaluated with a disease duration of 10 years, he suffered from severe motor fluctuations and freezing of gait, accompanied by severe non-motor symptoms, including dementia, visual hallucinations, delusions, depression, RBD, and orthostatic hypotension. He scored 48 on the UPDRS III score (off) and only 7/30 on the MMSE. The other brother (II.3) was diagnosed with PD at age 62 years and died at age 67 years.

Haplotype Analysis: Sharing 1.1 Mb Region

Haplotye analysis showed that PD patients carrying the A30G mutation from these three families shared at least a 1.1 Mb region spanning from rs9993181 to rs34001515 (see Table S1).

Structure of A30G αSyn

To investigate the molecular and functional consequences of the A30G mutation in αSyn, we recombinantly prepared wild-type (WT) αSyn as well as the A30G mutant. For both proteins, the molecular structure, the ability to bind to membranes, and aggregation into amyloid fibrils were analyzed using a combination of biophysical methods. Both proteins displayed small signal spread in two-dimensional NMR $^{1}H/^{15}N$-correlation spectra, indicative of intrinsically disordered proteins (Fig. 3a). Most cross peaks overlapped for the two proteins with the exception of cross peaks belonging to residues in close proximity to the mutation site (Fig. 3a). Sequence-specific analysis showed that the perturbations in NMR signal intensity and position were localized around the mutation site (Fig. 3b).

Next, we analyzed the secondary structure of A30G αSyn. To this end, we combined NMR spectroscopy with MD simulations. In $^{1}H/^{13}C$-correlation spectra, we observed a small downfield/upfield shift in the $^{1}H/^{13}C$ dimension for selected Hα/Cα cross peaks (Fig. 3c), which is characteristic of a decrease in α-helical propensity. To gain further insight into the influence of the A30G mutation on the local conformation of αSyn, we performed MD simulations of the αSyn peptide K23-V37 either containing the WT alanine or a glycine at position 30. Analysis of the α-helical content observed

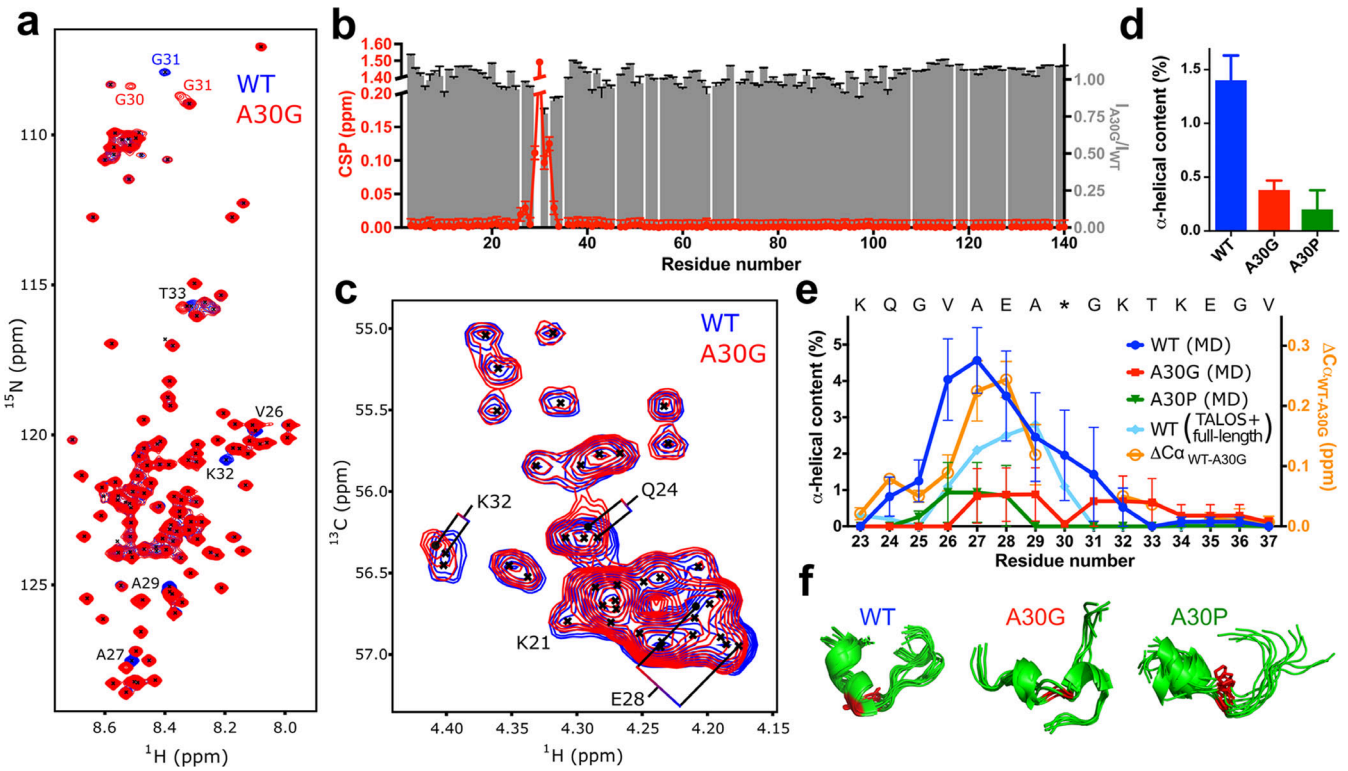

FIG. 3. A30G mutation decreases locally α-synuclein (αSyn)'s α-helical propensity. (**a**) $^{1}H/^{15}N$-HMQC of wild type (WT, blue) and A30G mutant (red) αSyn. The most perturbed residues are labeled. (**b**) N-HN chemical shift perturbations (red) and intensity ratios (gray) between WT and A30G αSyn based on the spectrum in (**a**). (**c**) Selected region of the $^{1}H/^{13}C$ HSQC of WT (blue) and A30G (red) αSyn. The affected residues are labeled. (**d**) α-Helical content of WT and A30G αSyn, as well as A30P αSyn for comparison, over the molecular dynamics (MD) simulation of 10 ns. Error bars indicate the standard error from the 15 analyzed peptides. (**e**) Residue-specific α-helical content for WT (blue) and mutant αSyn (red, green) over the 10 ns MD simulation together with the calculated secondary structure from the chemical shifts (light blue) by TALOS+ (BMRB id: 25227). In addition, the difference between the Cα chemical shifts of WT and A30G αSyn is shown (orange; displayed on the right axis). Error bars indicate the standard error from the 15 peptides analyzed (MD) and the estimated chemical shift error. (**f**) Example structures from the simulations that present α-helical structure. Ten structures from two different simulations were aligned for each peptide. Residue 30 is highlighted in red. [Color figure can be viewed at wileyonlinelibrary.com]

during the MD simulation showed that in both peptides α-helical conformations were only occasionally sampled (Fig. 3d). In the case of the A30G mutant, however, the α-helical propensity was further decreased by a factor of 3–4 when compared to WT αSyn (Fig. 3d). Calculations performed in parallel for the genetic mutation A30P revealed a similar decrease in α-helical propensity (Fig. 3d). Residue-specific analysis showed that in the WT peptide the α-helical tendency peaks at V26-A29 (Fig. 3e; blue) were consistent with α-helical propensity calculated in this region from the experimental NMR chemical shifts of the full-length protein (Fig. 3e; light blue). In contrast, V26-A29 assumed more rarely α-helical conformations in the A30G, as well as A30P, mutant chain. The strongest differences between the Ca chemical shifts of WT and A30G mutant αSyn were also observed for residues V26-A29 (Fig. 3e; orange). Selected snapshots from the MD simulations displaying α-helical structure are shown in Fig. 3f. The combined analysis showed that the A30G mutation decreased locally αSyn's α-helical propensity. The perturbation of α-helical structure is in agreement with the known amino acid properties of alanine and glycine: alanine is the residue that most strongly favors α-helix formation, while glycine residues are often found in turns.[26] Indeed, due to the replacement of alanine by glycine at position 30, two glycines are now present at positions 30 and 31, strongly promoting the local flexibility of the αSyn polypeptide backbone.

A30G αSyn Binding to Lipid Vesicles

To investigate the ability of A30G αSyn to interact with membranes, we prepared liposomes from a mixture of DOPE:DOPS:DOPC (5:3:2 w/w). Increasing liposome concentrations were titrated to WT, A30G, and A30P αSyn. Previous studies have shown that upon binding of αSyn to liposomes, the formation of the membrane-bound, α-helical conformation can be monitored by CD. For all three proteins, we observed a liposome-induced transition from a random coil conformation to α-helical structure (Fig. 4a). For WT and A30G αSyn, a defined isosbestic point (wavelength

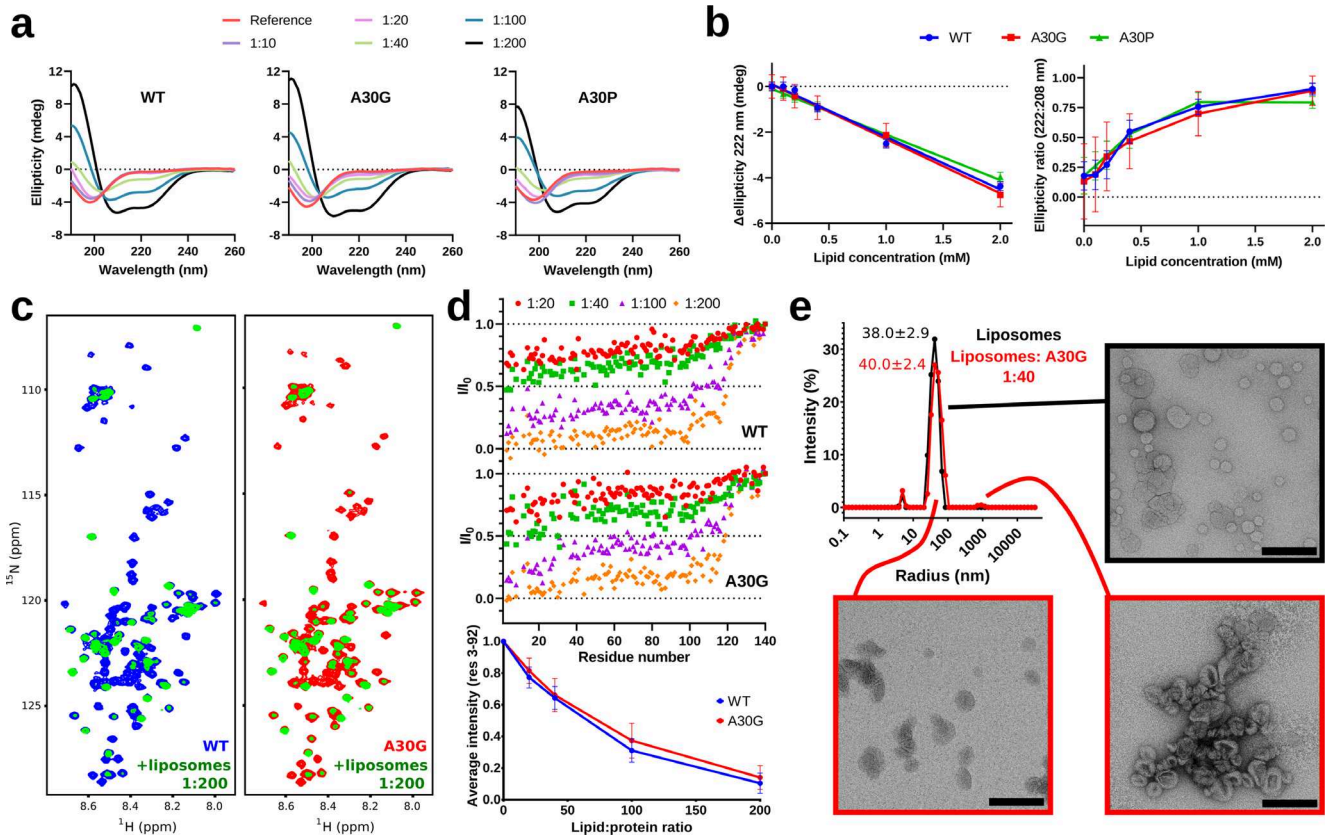

FIG. 4. A30G α-synuclein (αSyn) binds to lipid bilayers. (**a**) Circular dichroism experiments of wild type (WT), A30G, and A30P αSyn at different protein: lipid ratios. (**b**) Change in ellipticity at 222 nm (left) and change in the ellipticity ratio between 222 and 208 nm (right) upon increasing concentrations of lipid for WT (blue), A30G (red), and A30P (green) indicating an increase of α-helical structure. (**c**) $^{1}H/^{15}N$-HMQC of WT (blue, left) and A30G mutant (red, right) αSyn compared with the respective proteins in the presence of liposomes with a protein:lipid ratio of 1:200 (green). (**d**) Residue-specific $^{1}H/^{15}N$-HMQC peak intensity ratios at increasing protein:lipid ratios for WT (top) and A30G (bottom) αSyn. In the lower panel, changes in the average intensity of the cross peak signals of residues 3–92 for increasing liposome concentrations are shown for WT (blue) and A30G (red) αSyn, respectively. Error bars represent standard deviations. (**e**) Dynamic light scattering experiments of liposomes (black) and liposomes in presence of A30G αSyn at 1:40 protein: lipid ratio (red). Electron microscopy pictures of liposomes alone (black), liposomes in the presence of A30G (red, left), and accumulates of liposomes in presence of A30G αSyn (red, right) are displayed. Scale bars = 200 nm. [Color figure can be viewed at wileyonlinelibrary.com]

around 203–204 nm) was present, which was perturbed in the case of A30P αSyn (Fig. 4a). Analysis of the change in ellipticity at 222 nm and the change in the ellipticity ratio between 222 and 208 nm for increasing lipid concentrations further supported the increase in α-helical structure (Fig. 4b). In addition, the analysis pointed to slight differences in the binding process of A30G and A30P αSyn to DOPE:DOPS:DOPC liposomes when compared to WT αSyn (Fig. 4b).

To gain residue-specific insight into the binding of A30G αSyn to membranes, we monitored the $^{1}H/^{15}N$ NMR signals of A30G αSyn in the presence of increasing liposome concentrations (Fig. 4c). Because liposomes have a high molecular weight, only the residual unbound protein will be observed in $^{1}H/^{15}N$ correlation spectra.[27] With increasing liposome concentration, an increasing fraction of αSyn molecules was bound to the liposomes such that the NMR signal intensity gradually decreased (Fig. 4c,d). Residue-specific analysis, however, showed that αSyn did not bind uniformly as a single entity to membranes, but different αSyn regions had specific interaction modes.[28-30] The most liposome-perturbed region comprises the N-terminal residues up to approximately E20 (Fig. 4d), which acts as a membrane anchor in αSyn.[28,29] A further gradual increase in signal intensity in the presence of liposomes was observed for residues up to ~90–100, followed by another less broadened region up to ~118 (Fig. 4d). The C-terminal 10–20 residues were not broadened even at the highest liposome concentrations (Fig. 4d), indicating that they remained unbound and highly flexible. In agreement with the CD spectra, the residue-specific broadening profile of A30G αSyn was similar to that of the WT protein (Fig. 4d). Specific analysis of the liposome-induced signal broadening of residues 3–92, that is, the liposome-binding region, furthermore suggested a slight perturbation of the binding of A30G αSyn to membranes (lower panel in Fig. 4d). Finally, we noted that A30G αSyn promoted the clustering of vesicles as evidenced by dynamic light scattering and electron microscopy (Fig. 4e).

Amyloid-like Fibril Formation of αSyn and its A30G Mutant

Because aggregation of αSyn into insoluble deposits is the pathological hallmark of PD,[31] we next studied the aggregation behavior of A30G αSyn and compared it to the WT protein as well as the A30P mutant. The three proteins were incubated individually and amyloid fibril formation was monitored using Thioflavin-T fluorescence (Fig. 5a). In agreement with previous studies,[32] the A30P mutation slowed down the kinetics of αSyn fibrillization when compared to the WT protein (Fig. 5a), although amyloid fibrils were observed for both proteins by electron microscopy (Fig. 5b). In

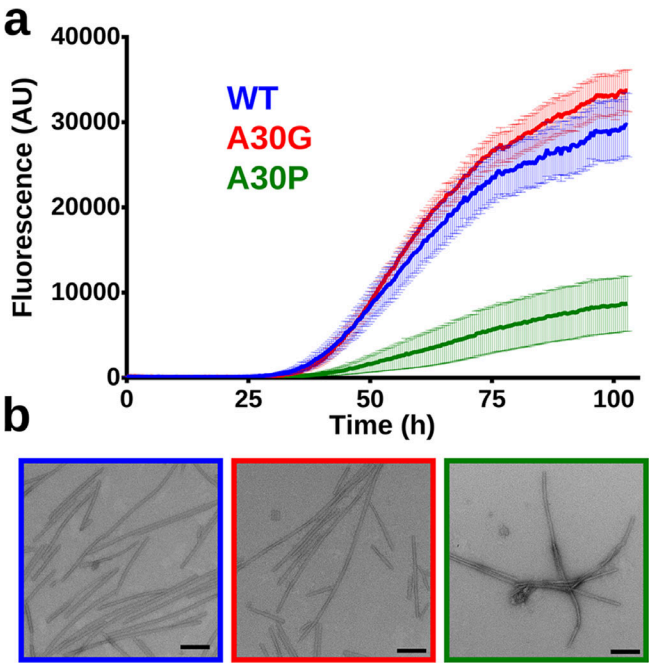

FIG. 5. Amyloid-like fibril formation of α-synuclein (αSyn) and its A30G mutant. (**a**) Aggregation kinetics of wild type (WT) (blue) and A30G (red) αSyn measured by Thioflavin-T fluorescence at 37°C. The delayed aggregation kinetics of A30P αSyn (green) are shown for comparison. (**b**) Electron microscopy pictures of WT (blue), A30G (red), and A30P (green) αSyn fibrils. Scale bars = 200 nm. [Color figure can be viewed at wileyonlinelibrary.com]

strong contrast to the A30P mutation, however, A30G αSyn did not aggregate slower, but had similar aggregation kinetics than WT αSyn, while also generating more Thioflavin-T fluorescence (Fig. 5a). The stronger Thioflavin-T fluorescence could either be caused by more amyloid fibrils being formed or mutation-induced changes in the conformation of A30G αSyn amyloid fibrils (Fig. 5a).

Discussion

Here, we describe clinical and genetic findings in carriers of a SNCA A30G founder mutation from three different Greek families as well as the functional consequences of this variant on αSyn conformation, lipid binding, and aggregation. Based on the identification of A30G co-segregating with the disease in three families, the absence of the mutation in controls and population databases, the conservation of A30 residue across species, and the predicted and observed functional effects, we propose SNCA A30G as a novel causative mutation. This mutation is responsible for a PD phenotype characterized by AAO varying widely (36–80 years), a good initial response to levodopa, motor fluctuations, and prominent non-motor symptoms, like cognitive decline, orthostatic hypotension, RBD, hallucinations, and various psychiatric manifestations.

It should be noted that the index patient's father (II.4) from family B at age 80 years had very mild motor symptoms and did not fulfil the recently developed MDS PD diagnostic criteria, which suggests that A30G might have incomplete penetrance. Given, however, the constellation of motor and non-motor symptoms and signs, it is very likely that he will fulfil such criteria in the near future. In Family C, the index patient's parents passed away a long time ago, so we do not know if one would have developed PD. Given the segregation of the heterozygous A30G variant in all families, however, we think that also in family C an autosomal dominant pattern of inheritance is the most likely explanation. We also observed a founder effect of the SNCA A30G mutation. This indicates that the A30G mutation could be important for PD development in the Greek population and should be regularly screened in dominant PD cases in Greece. In our previous work, we found that the SNCA A53T mutation was responsible for 5.5% of the Greek familial PD population,[33] while the percentage is even higher for those with combined dominant family history and age of onset below the age of 50 years. Therefore, the A53T and the A30G SNCA mutations should be regularly sought after in Greek PD cases with family history, especially in those with early age of onset.

The mean AAO for these three A30G families was 58 ± 12 years and the other mutation at this A30 residue (A30P) found in one German family[34] caused a similar AAO (59.7 ± 10.8 years). Carriers with A30P or A30G all present with classical Parkinsonian motor dysfunction and good response to levodopa, but A30G carriers appear to generally develop more non-motor symptoms, in particular dementia, hallucinations, orthostatic hypotension, RBD, and psychiatric manifestations. Interestingly, visual hallucinations and autonomic dysfunction were also manifested in G51D cases with variable AAO and pyramidal signs.[13,35] SNCA E46K mutation was first reported in a family of Spanish origin, with severe parkinsonism and dementia with Lewy bodies (DLB)[10] and then it was found in a Bolivian family with a less aggressive phenotype and without dementia,[11] which indicated phenotypic heterogeneity in PD patients with the same mutation. The A53E mutation in SNCA results in hypokinetic-rigid PD with early-onset (AAO, 34.3 ± 8.6 years), prominent levodopa-induced dyskinesia, but without cognitive decline.[15] Patients with the A53T mutation, the most common SNCA missense mutation, have a phenotype resembling idiopathic PD, but with a generally earlier AAO (mean of 45 years of age) and a more severe disease course, including prominent non-motor features, such as dementia and autonomic dysfunction.[36,37]

It is noteworthy that the A30P mutation has only been identified in one family with autosomal dominant PD, which has raised some doubts about its pathogenicity. The fact that we have now identified another mutation at the A30 site in three unrelated families reinforces the importance of this site and the pathogenic potential of amino acid substitutions in this residue.

The biophysical analysis showed that the A30G mutation had a local effect on the intrinsically disordered structure of αSyn,[38,39] decreasing the α-helical propensity of residues V26-A29 (Fig. 3). We further demonstrated that A30G αSyn binds to lipid bilayers (Fig. 4). The binding is comparable to that of WT αSyn (Fig. 4), although both CD and NMR spectroscopy suggested a slight perturbation of membrane binding caused by the A30G mutation. A30G and A30P are located in the first helical fragment of the N-terminal domain[40] (Fig. 2d). Previous studies have shown that – among the known genetic mutations in αSyn – A30P most strongly affects αSyn's ability to interact with membranes.[27,41-44] However, even in the case of the A30P mutation, there is only an ~1 kcal/mol difference in free energy in the interaction of A30P αSyn binding to large and small unilamellar vesicles when compared to the E46K mutant protein, which binds slightly stronger to membranes than WT αSyn.[41] The data suggest that the decrease in α-helical propensity of residues V26-A29 does not block membrane binding and formation of α-helical structure, but disfavors it. Differences in membrane binding of αSyn mutants are thus likely to be influenced by the lipid composition of membranes, as well as membrane curvature. Indeed, a recent study using sodium dodecyl sulfate (SDS)-coated gold nanoparticles reported similar binding affinities for WT, A30P, and E46K αSyn and suggested that membrane deformability might contribute to the αSyn/membrane interaction.[45]

Because the aggregation of αSyn into insoluble deposits is tightly connected to PD and other synucleinopathies, we investigated whether the A30G mutation impacted amyloid fibril formation of αSyn. We found that replacement of alanine by glycine at position 30 resulted in higher Thioflavin-T fluorescence, a signature of increased fibril formation or differences in fibril structure (Fig. 5). The aggregation behavior of A30G αSyn was in contrast to the A30P mutation, which strongly delays αSyn fibrillization, but might at the same time allow enhanced protein oligomerization.[32] The finding that the A30G mutation slightly perturbed membrane binding and promoted fibril formation/changed fibril structure is also quite unique among the known SNCA missense mutations, because other mutations either have no effect on one of the two processes (ie, membrane binding or fibrillization) or even have opposite effects such as the E46K mutation, which enhances membrane binding.[41,43] The A30G mutation thus might cause a double-hit effect, in which the equilibrium between membrane-bound and soluble protein is biased towards the soluble protein, which then also aggregates more strongly in the cytosol

when compared to WT αSyn. This double-hit effect might explain the more severe phenotype than the one caused by A30P. Although the perturbations introduced by the A30G mutation might appear small, they can accumulate in neurons over the long periods during which PD develops.

In conclusion, we identified a novel heterozygous SNCA A30G mutation causing familial PD with various prominent non-motor symptoms. The mutation altered the α-helical structure of the protein, perturbed membrane binding, and promoted fibril formation. These novel genetic and functional data shed new light on the mechanisms through which aberrant αSyn may lead to PD and are relevant for the common form of idiopathic PD, in which αSyn alterations are thought to play a prominent role.

Acknowledgments: We thank M. Wegstroth for protein preparation and the EM facility of the Max Planck Institute for Biophysical Chemistry for electron micrographs. The obtaining of patient information and of biological material was performed under protocols approved by the Scientific Committees of the "Attikon" and "Eginition" Hospitals, and all subjects signed relevant consent forms.

References

1. Poewe W, Seppi K, Tanner CM, et al. Parkinson disease. Nat Rev Dis Primers 2017;3:1–21.
2. Xu L, Pu J. Alpha-Synuclein in Parkinson's disease: from pathogenetic dysfunction to potential clinical application. Parkinsons Dis 2016;2016:1720621.
3. Polymeropoulos MH, Lavedan C, Leroy E, et al. Mutation in the α-synuclein gene identified in families with Parkinson's disease. Science 1997;276:2045–2047.
4. Klein C, Westenberger A. Genetics of Parkinson's disease. Cold Spring Harb Perspect Med 2012;2:a008888.
5. Proukakis C, Dudzik CG, Brier T, et al. A novel α-synuclein missense mutation in Parkinson disease. Neurology 2013;80:1062–1064.
6. Appel-Cresswell S, Vilarino-Guell C, Encarnacion M, et al. Alpha-synuclein p.H50Q, a novel pathogenic mutation for Parkinson's disease. Mov Disord 2013;28:811–813.
7. Blauwendraat C, Kia DA, Pihlstrom L, et al. Insufficient evidence for pathogenicity of SNCA His50Gln (H50Q) in Parkinson's disease. Neurobiol Aging 2018;64:159.e5–159.e8.
8. Yoshino H, Hirano M, Stoessl AJ, et al. Homozygous alpha-synuclein p.A53V in familial Parkinson's disease. Neurobiol Aging 2017;57:248.e7–248.e12.
9. Chen Y, Gu X, Ou R, et al. Evaluating the role of SNCA, LRRK2, and GBA in Chinese patients with early-onset Parkinson's disease. Mov Disord 2020;35:2046–2055. https://doi.org/10.1002/mds.28191
10. Zarranz JJ, Alegre J, Gómez-Esteban JC, et al. The new mutation, E46K, of alpha-synuclein causes Parkinson and Lewy body dementia. Ann Neurol 2004;55:164–173.
11. Pimentel MMG, Rodrigues FC, Leite MAA, et al. Parkinson disease: α-synuclein mutational screening and new clinical insight into the p.E46K mutation. Parkinsonism Relat Disord 2015;21:586–589.
12. Lesage S, Anheim M, Letournel F, et al. G51D α-synuclein mutation causes a novel Parkinsonian–pyramidal syndrome. Ann Neurol 2013;73:459–471.
13. Kiely AP, Ling H, Asi YT, et al. Distinct clinical and neuropathological features of G51D SNCA mutation cases compared with SNCA duplication and H50Q mutation. Mol Neurodegener 2015;10:41.
14. Pasanen P, Myllykangas L, Siitonen M, et al. Novel α-synuclein mutation A53E associated with atypical multiple system atrophy and Parkinson's disease-type pathology. Neurobiol Aging 2014;35:2180.e1–2180.e5.
15. Martikainen MH, Päivärinta M, Hietala M, Kaasinen V. Clinical and imaging findings in Parkinson disease associated with the A53E SNCA mutation. Neurol Genet 2015;1:e27.
16. Krüger R, Kuhn W, Müller T, et al. Ala30Pro mutation in the gene encoding alpha-synuclein in Parkinson's disease. Nat Genet 1998;18:106–108.
17. Postuma RB, Berg D, Stern M, et al. MDS clinical diagnostic criteria for Parkinson's disease. Mov Disord 2015;30:1591–1601.
18. Goetz CG, Fahn S, Martinez-Martin P, et al. Movement Disorder Society-sponsored revision of the Unified Parkinson's Disease Rating Scale (MDS-UPDRS): process, format, and clinimetric testing plan. Mov Disord 2007;22:41–47.
19. Hoehn MM, Yahr MD. Parkinsonism: onset, progression and mortality. Neurology 1967;17:427–442.
20. Nasreddine ZS, Phillips NA, Bédirian V, et al. The Montreal Cognitive Assessment, MoCA: a brief screening tool for mild cognitive impairment. J Am Geriatr Soc 2005;53:695–699.
21. Folstein MF, Folstein SE, McHugh PR. "Mini-mental state". A practical method for grading the cognitive state of patients for the clinician. J Psychiatr Res 1975;12:189–198.
22. McLaren W, Gil L, Hunt SE, et al. The Ensembl Variant Effect Predictor. Genome Biol 2016;17:122.
23. Schwarz JM, Cooper DN, Schuelke M, Seelow D. MutationTaster2: mutation prediction for the deep-sequencing age. Nat Methods 2014;11:361–362.
24. Sim N-L, Kumar P, Hu J, Henikoff S, Schneider G, Ng PC. SIFT web server: predicting effects of amino acid substitutions on proteins. Nucleic Acids Res 2012;40:W452–W457.
25. Rentzsch P, Witten D, Cooper GM, Shendure J, Kircher M. CADD: predicting the deleteriousness of variants throughout the human genome. Nucleic Acids Res 2019;47:D886–D894.
26. Chou PY, Fasman GD. Prediction of protein conformation. Biochemistry 1974;13:222–245.
27. Bodner CR, Maltsev AS, Dobson CM, Bax A. Differential phospholipid binding of α-synuclein variants implicated in Parkinson's disease revealed by solution NMR spectroscopy. Biochemistry 2010;49:862–871.
28. Bodner CR, Dobson CM, Bax A. Multiple tight phospholipid-binding modes of α-synuclein revealed by solution NMR spectroscopy. J Mol Biol 2009;390:775–790.
29. Fusco G, De Simone A, Gopinath T, et al. Direct observation of the three regions in α-synuclein that determine its membrane-bound behaviour. Nat Commun 2014;5:3827.
30. Eliezer D, Kutluay E, Bussell R, Browne G. Conformational properties of alpha-synuclein in its free and lipid-associated states. J Mol Biol 2001;307:1061–1073.
31. Stefanis L. α-Synuclein in Parkinson's disease. Cold Spring Harb Perspect Med 2012;2:a009399.
32. Conway KA, Lee S-J, Rochet J-C, Ding TT, Williamson RE, Lansbury PT. Acceleration of oligomerization, not fibrillization, is a shared property of both α-synuclein mutations linked to early-onset Parkinson's disease: implications for pathogenesis and therapy. Proc Natl Acad Sci U S A 2000;97:571–576.
33. Bozi M, Papadimitriou D, Antonellou R, et al. Genetic assessment of familial and early-onset Parkinson's disease in a Greek population. Eur J Neurol. 2014;21:963–968.
34. Krüger R, Kuhn W, Leenders KL, et al. Familial parkinsonism with synuclein pathology: clinical and PET studies of A30P mutation carriers. Neurology 2001;56:1355–1362.
35. Deng H, Wang P, Jankovic J. The genetics of Parkinson disease. Ageing Res Rev 2018;42:72–85.
36. Papadimitriou D, Antonelou R, Miligkos M, et al. Motor and non-motor features of carriers of the p.A53T alpha-synuclein mutation: a longitudinal study. Mov Disord 2016;31:1226–1230.

37. Koros C, Stamelou M, Simitsi A, et al. Selective cognitive impairment and hyposmia in p.A53T SNCA PD vs typical PD. Neurology 2018;90:e864–e869.

38. Bertoncini CW, Jung Y-S, Fernandez CO, et al. Release of long-range tertiary interactions potentiates aggregation of natively unstructured alpha-synuclein. Proc Natl Acad Sci U S A 2005;102: 1430–1435.

39. Weinreb PH, Zhen W, Poon AW, Conway KA, Lansbury PT. NACP, a protein implicated in Alzheimer's disease and learning, is natively unfolded. Biochemistry 1996;35:13709–13715.

40. Ulmer TS, Bax A, Cole NB, Nussbaum RL. Structure and dynamics of micelle-bound human alpha-synuclein. J Biol Chem 2005;280: 9595–9603.

41. Middleton ER, Rhoades E. Effects of curvature and composition on α-synuclein binding to lipid vesicles. Biophys J 2010;99:2279–2288.

42. Nuscher B, Kamp F, Mehnert T, et al. α-Synuclein has a high affinity for packing defects in a bilayer membrane a thermodynamics study. J Biol Chem 2004;279:21966–21975.

43. Stöckl M, Fischer P, Wanker E, Herrmann A. α-Synuclein selectively binds to anionic phospholipids embedded in liquid-disordered domains. J Mol Biol 2008;375:1394–1404.

44. Karpinar DP, Balija MBG, Kügler S, et al. Pre-fibrillar α-synuclein variants with impaired β-structure increase neurotoxicity in Parkinson's disease models. EMBO J 2009;28:3256–3268.

45. McClain SM, Ojoawo AM, Lin W, Rienstra CM, Murphy CJ. Interaction of alpha-synuclein and its mutants with rigid lipid vesicle mimics of varying surface curvature. ACS Nano 2020;14: 10153–10167.

Supporting Data

Additional Supporting Information may be found in the online version of this article at the publisher's web-site.